1.55 μm ultrafast photoconductive switches based on ErAs:InGaAs

F. Ospald,[1] D. Maryenko,[1] K. von Klitzing,[1] D. C. Driscoll,[2] M. P. Hanson,[2] H. Lu,[2] A. C. Gossard,[2] and J. H. Smet[1]

[1]*Max-Planck-Institut für Festkörperforschung, Heisenbergstraße 1, 70569 Stuttgart, Germany*
[2]*Materials Department, University of California-Santa Barbara, Santa Barbara, California 93106-5050, USA*

(Received 16 January 2008; accepted 17 March 2008; published online 3 April 2008)

The electron capture time in superlattice structures consisting of periodically spaced layers of self-assembled ErAs nanoislands and $In_{0.53}Ga_{0.47}As$ is investigated on photoconductive switches as a function of the superlattice period using photocurrent autocorrelation and pulsed laser excitation at 1.55 μm. The capture time can be tuned from picoseconds all the way down to 0.2 ps by changing the periodicity. Two different Be doping schemes are explored to reduce the dark current. The resulting characteristics indicate that ErAs:InGaAs may serve as a high performance photoconductive material at this wavelength for pulsed terahertz emission and detection. © *2008 American Institute of Physics*. [DOI: 10.1063/1.2907335]

Low-temperature-grown (LTG) GaAs is a well-established ultrafast photoconductive material for generating and detecting pulsed terahertz radiation.[1,2] Due to its room temperature bandgap of 1.42 eV, efficient excitation demands illumination with wavelengths $\leqslant 0.87$ μm. The possibility to use inexpensive and maintenance-free pulsed fiber laser systems with a small footprint would significantly contribute to the proliferation of imaging applications based on pulsed terahertz radiation. Such lasers operate at the telecommunication wavelength of 1.55 μm and require a suitable alternative to LTG-GaAs with lower bandgap. $In_{0.53}Ga_{0.47}As$ lattice matched to InP covers the proper wavelength range and is expected to yield higher terahertz output because of its higher electron mobility.[3] In order to reduce the carrier lifetime of $In_{0.53}Ga_{0.47}As$ to the (sub)picosecond level, nonradiative defects have been introduced either by growing at low temperature[4–6] or by ion bombardment.[7–9] In this letter, we investigate $In_{0.53}Ga_{0.47}As$ in which ErAs island layers are embedded to form a periodic superlattice of ErAs and $In_{0.53}Ga_{0.47}As$. The ErAs islands act as efficient trap sites.[10] The lifetimes of photogenerated charge carriers in this material class are determined from photocurrent autocorrelation measurements on photoconductive switches. This method has the advantage that it is closest to how switches are operated in terahertz applications. Apart from offering exceptional lifetime tunability down to 0.2 ps through a variation of the superlattice period, similar to what has been observed on ErAs:GaAs,[11,12] this material also offers competitive dark resistivities in comparison to other contenders at 1.55 μm such as those in Refs. 4–9.

The ErAs:InGaAs superlattices studied here were grown at 490 °C with molecular beam epitaxy on top of a semi-insulating (100) InP:Fe substrate and a 250 nm thick $In_{0.52}Al_{0.48}As$ buffer. A schematic cross section of the sample structure is depicted in Fig. 1(a). Each superlattice consists of a periodic sequence of a layer of self-assembled ErAs islands and an $In_{0.53}Ga_{0.47}As$ spacer of thickness L. The superlattice is terminated with an $In_{0.53}Ga_{0.47}As$ cap of the same thickness. Due to surface chemistry, ErAs deposited on top of $In_{0.53}Ga_{0.47}As$ forms nanometer-sized islands with an approximately constant height of 4 ML when an equivalent of 0.2–2 ML of ErAs is deposited.[13] The island layer can be overgrown with crystalline $In_{0.53}Ga_{0.47}As$. The incorporation of ErAs into $In_{0.53}Ga_{0.47}As$ shifts the Fermi level close to or above the conduction band edge and the superlattice behaves as n-type material. The dark resistivity can, however, be sig-

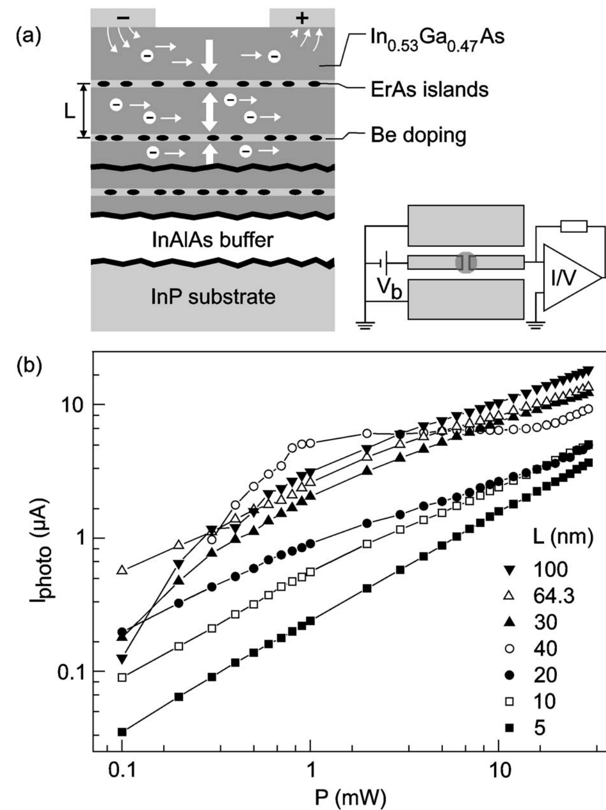

FIG. 1. (a) Top left panel: Vertical cross section of an ErAs:InGaAs superlattice. The lateral drift and vertical diffusion of photoexcited electrons are schematically illustrated. Top right panel: Top view of an illuminated photoconductive switch. The measurement circuitry has also been included. (b) Photocurrent as a function of the average incident laser power obtained on a set of seven superlattices of different periodicities for a bias voltage of 2.0 V.

[a]Electronic mail: j.smet@fkf.mpg.de.

Author complimentary copy. Redistribution subject to AIP license or copyright, see http://apl.aip.org/apl/copyright.jsp

nificantly enhanced by introducing p-type dopants to compensate. By appropriately adjusting the doping level, the Fermi energy can be tuned toward midgap.[14] Two sets of samples were investigated: Wafers with L ranging between 5 and 20 nm exhibit an active superlattice with a total thickness of 500 nm, an amount of ErAs per superlattice period equivalent to 0.8 ML, and Be δ-doping (local sheet density of 5×10^{13} cm^{-2}) in the immediate vicinity of the island layer to compensate for free electrons. Wafers with L from 30 to 100 nm have a 1200 nm thick active superlattice and 1.75 ML ErAs deposition per superlattice period. They contain a region uniformly doped with a local Be concentration of 1×10^{20} cm^{-3}, which extends 2.5 nm above and below each ErAs plane. This doping profile will be referred to as step doping. For photocurrent autocorrelation measurements, a coplanar waveguide, consisting of a 30 μm wide strip, which is separated from the ground planes by a 15 μm broad gap, was photolithographically patterned on top of these samples (10 nm Ti adhesion layer, 200 nm Au metallization). The photoconductive switch is a 3 μm wide gap in the central conductor. A top view of the geometry and the measurement circuit is shown in Fig. 1(a).

Photocurrents in these ErAs:$In_{0.53}Ga_{0.47}As$ switches show a sublinear dependence on the illumination intensity, i.e., the density of photoexcited charge carriers. The photocurrent dependence on the average optical power incident on the switch P is shown in Fig. 1(b). With the exception of the superlattice with a 40 nm period, all wafers with L larger than 10 nm follow a power law $I_{photo}\propto P^{\alpha}$ with $\alpha=0.5\pm0.1$. The sublinearity was somewhat less pronounced for the 5 and 10 nm superlattices ($0.65<\alpha<0.80$). The more complex behavior in the 40 nm sample probably originates from deviations from the optimum Be doping level. Measurements on a set of wafers with constant L and ErAs deposition (not shown here) but varying Be concentration exhibited both types of photocurrent curves. The photocurrent nonlinearity can be exploited to determine the capture time of photoexcited charge carriers using autocorrelation techniques.[15] We use the setup of Fig. 2(a). It is analogous to a Mach–Zehnder interferometer. An optical parametric oscillator, pumped with a mode-locked Ti:sapphire laser (Coherent) emits pulses of ~150 fs duration at 76 MHz repetition frequency. The pulse train is split into two parts of equal intensity. One beam path comprises a retroreflector mounted on a stepper motor for zero-delay adjustment, the other beam path contains a retroreflector oscillating at a low but fixed frequency (~10 Hz). This so-called shaker produces a sinusoidally varying time delay between the two beams with an amplitude of ±25 ps. After cross polarizing the beams, they are collinearly superimposed and focused onto the photoconductive switch with a 100× microscope objective. The photocurrent flowing across the biased switch is amplified and recorded with an oscilloscope as a function of the delay time τ. The intensity noise of the laser system is suppressed by averaging over multiple delay cycles of the shaker. We neglect the photocurrent contribution of the holes in view of their much lower mobility.[16] The time evolution of the photoexcited electron population is approximated with a Taylor series up to the second order.[15] The assumption of a single exponential to describe the decay of the photoexcited charge population then allows the derivation of a fit function, which contains the electron capture or lifetime τ_e as fit parameter[12] [see Fig. 2(b)]. For lifetimes shorter than ~400 fs, a technique based on short-distance pulse propagation on a coplanar stripline was used instead to avoid complications associated with the polarizing effect (similar to a wire grid) of the gap geometry as described in Ref. 12. This so-called sliding-contact method yields a double-peak signal centered around zero delay. It can be fitted to a function containing τ_e, which results from the convolution between the laser induced charge carrier population at the switch and the carrier lifetime broadened pulse, which has propagated a distance of 150 μm.

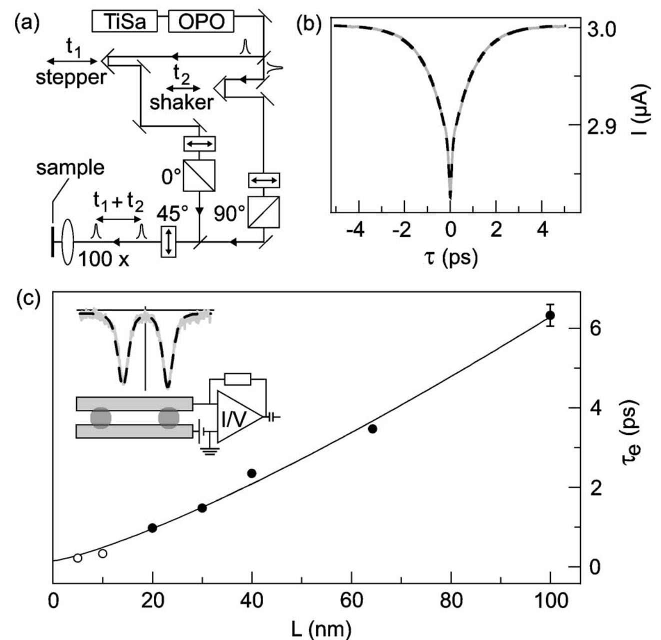

FIG. 2. (a) Setup for photocurrent autocorrelation experiments. (b) Typical autocorrelation trace for a bias voltage of 2.0 V and an average optical power per beam path of 2.0 mW. The dip results from the photocurrent sublinearity. The extracted lifetime τ_e in this case is 943 fs. (c) Lifetime τ_e of photoexcited electrons as a function of the ErAs:InGaAs superlattice period L. The solid line is a power-law fit with exponent 1.26: $\tau_e=L^{1.26}/53.7+0.15$ ps with L in nanometer. Data for $L>10$ nm (solid circles) were obtained from autocorrelation experiments. The upper inset shows the measurement geometry, a typical trace and fit for sliding-contact measurements. This propagation technique was applied for the 5 and 10 nm superlattices (open circles).

The main panel of Fig. 2(c) displays the extracted lifetimes as a function of the superlattice period. The smallest τ_e was measured on the 5 nm wafer and was 220 fs. This is still larger than the estimated time resolution of our setup. Previous studies on ErAs:GaAs superlattices at 800 nm indicated that the electron capture process is governed by diffusion of the excited carriers to the ErAs island layers. This manifests itself in a quadratic dependence of τ_e on L.[11,12] The electron capture is a two-step process. The steep carrier density gradients due to Beer's absorption law and trapping at the ErAs layers force the photoexcited carriers toward the ErAs planes. As they impinge on the ErAs island, they are captured. The time scale of the second step appears negligibly small compared to the average time that elapses between excitation of the electron and its arrival at an ErAs island. Note that the electric field applied across the gap predominantly causes in-plane charge carrier drift whereas the vertical motion is diffusion driven. The data in Fig. 2(c) have been analyzed with this model in mind. They are fitted with

Author complimentary copy. Redistribution subject to AIP license or copyright, see http://apl.aip.org/apl/copyright.jsp

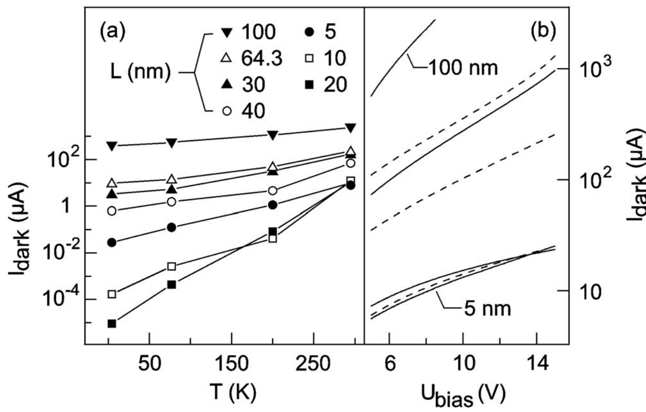

FIG. 3. (a) Dark currents in the wafers of this study for a bias voltage of 8.0 V at 4.2, 77, 200, and 295 K. (b) Dark currents at room temperature in a voltage range suitable for terahertz applications for superlattice periods (from top to bottom) of 100, 64.3, 30, 40, 10, 20, and 5 nm.

$$\tau_e = \frac{L^\gamma}{D} + \tau_L. \tag{1}$$

Here, τ_e is the calculated electron lifetime, L the superlattice period, γ is the exponent of the power law dependence, D is an "effective" ambipolar diffusion coefficient, and the constant offset τ_L takes into account the nonzero laser pulse width of 150 fs in our setup. For a purely diffusive capture process, γ would take on a value of two and D would be equal to the ambipolar diffusion coefficient D^* (determined by the harmonic mean of the electron and hole mobility) multiplied with a factor π^2.[12] The fit yields $\gamma=1.26$ instead of $\gamma=2$ as expected.

There are several limitations to the diffusion-governed lifetime model that may cause the observed deviation from a quadratic dependence on the superlattice period. The most important one is no doubt the assumption of a constant ambipolar diffusion coefficient D^* for all wafers, which is not justified. The electron mobility in ErAs:InGaAs superlattices changes with the deposited amount of ErAs, the Be concentration, as well as the island layer spacing L.[10] The hole mobility is expected to change with these parameters as well. It is plausible that diffusion is enhanced for larger superlattice periods, which indeed would result in a slower increase of the electron lifetime as the superlattice period is increased. Also neglected is the outdiffusion of Be into the InGaAs bulk. Be has been previously used in LTG-InGaAs to create trap sites, and hence, trapping of charge carriers may not be restricted to the island layers.[5]

The usage of ErAs:$In_{0.53}Ga_{0.47}As$ superlattices as sources or detectors of broadband terahertz radiation not only requires short capture times but also low dark currents to yield a good signal-to-noise ratio and to prevent unnecessary heating of the device. $In_{0.53}Ga_{0.47}As$-based devices commonly display lower resistivities in comparison to GaAs-based structures due to the bandgap difference. Developing methods to reduce the dark current is therefore crucial. Here, we compare the two different Be doping schemes for compensation of the background electrons in our wafers. Figure 3(a) displays the dark current measured at a bias voltage of 8.0 V over a temperature range from liquid helium to room temperature. At all temperatures, the Be δ-doped wafers (with 5, 10, and 20 nm periodicities) exhibit dark currents at least one order of magnitude lower than wafers with step doping. This statement also holds across a voltage range where these photoconductive switches are usually operated in terahertz applications [see the room temperature measurement in Fig. 3(b)]. Besides the superior combination of a moderate ErAs deposition and the δ-doping profile for dark current reduction, the resistivity in the wafers with small L is additionally enhanced via the increased overlap of the depletion zones that are formed around the ErAs layers due to the compensation doping.[14] Van der Pauw measurements on our samples indicated room temperature dark resistivities of up to $3.43\times10^2\,\Omega$ cm for the δ-doped wafers. This value is comparable to the highest resistivities reached in LTG or ion-implanted $In_{0.53}Ga_{0.47}As$.[4,7,17]

The reported lifetimes in $In_{0.53}Ga_{0.47}As$-based photoconductive materials show a large spread from 0.2 to 1 ps,[4,6,7,9] which suggests the need for careful optimization and accurate control over growth parameters. In the case of ErAs:InGaAs, the lifetime is predominantly determined by the superlattice period. Therefore, ErAs:InGaAs with its high dark resistivity and exceptionally tunable lifetime down to at least 220 fs represents a very attractive and high performance photoconductive material for the emission and detection of broadband pulsed terahertz radiation using 1.55 μm glass fiber laser technology.

The authors would like to acknowledge contributions from E. Brown and financial support from DARPA TIFT, NSF MRSEC, and the BMBF NanoFutur program.

[1] A. C. Warren, N. Katzenellenbogen, D. Grischkowsky, J. M. Woodall, M. R. Melloch, and N. Otsuka, Appl. Phys. Lett. **58**, 1512 (1991).
[2] Y. C. Shen, P. C. Upadhya, H. E. Beere, E. H. Linfield, A. G. Davies, I. S. Gregory, C. Baker, W. R. Tribe, and M. J. Evans, Appl. Phys. Lett. **85**, 164 (2004).
[3] J. Lloyd-Hughes, E. Castro-Camus, and M. B. Johnston, Solid State Commun. **136**, 595 (2005).
[4] R. Takahashi, Y. Kawamura, T. Kagawa, and H. Iwamura, Appl. Phys. Lett. **65**, 1790 (1994).
[5] Y. Chen, S. S. Prabhu, S. E. Ralph, and D. T. McInturff, Appl. Phys. Lett. **72**, 439 (1998).
[6] K. Biermann, D. Nickel, K. Reimann, M. Woerner, T. Elsaesser, and H. Künzel, Appl. Phys. Lett. **80**, 1936 (2002).
[7] C. Carmody, H. H. Tan, C. Jagadish, A. Gaarder, and S. Marcinkevičius, Appl. Phys. Lett. **82**, 3913 (2003).
[8] M. Suzuki and M. Tonouchi, Appl. Phys. Lett. **86**, 051104 (2005).
[9] N. Chimot, J. Mangeney, L. Joulaud, P. Crozat, H. Bernas, K. Blary, and J. F. Lampin, Appl. Phys. Lett. **87**, 193510 (2005).
[10] D. C. Driscoll, M. P. Hanson, A. C. Gossard, and E. R. Brown, Appl. Phys. Lett. **86**, 051908 (2005).
[11] C. Kadow, S. B. Fleischer, J. P. Ibbetson, J. E. Bowers, A. C. Gossard, J. W. Dong, and C. J. Palmstrøm, Appl. Phys. Lett. **75**, 3548 (1999).
[12] M. Griebel, J. H. Smet, D. C. Driscoll, J. Kuhl, C. Alvarez Diez, N. Freytag, C. Kadow, A. C. Gossard, and K. von Klitzing, Nat. Mater. **2**, 122 (2003).
[13] D. C. Driscoll, M. P. Hanson, E. Mueller, and A. C. Gossard, J. Cryst. Growth **251**, 243 (2003).
[14] D. C. Driscoll, M. P. Hanson, and A. C. Gossard, J. Appl. Phys. **97**, 016102 (2005).
[15] T. F. Carruthers and J. F. Weller, Appl. Phys. Lett. **48**, 460 (1986).
[16] T. P. Pearsall and J. P. Hirtz, J. Cryst. Growth **54**, 127 (1981).
[17] A. Takazato, M. Kamakura, T. Matsui, J. Kitagawa, and Y. Kadoya, Appl. Phys. Lett. **90**, 101119 (2007).

Author complimentary copy. Redistribution subject to AIP license or copyright, see http://apl.aip.org/apl/copyright.jsp